Published in final edited form as:
Neuroimage. 2007 August 1; 37(1): 282–289. doi:10.1016/j.neuroimage.2007.04.055.

Neural responses to auditory stimulus deviance under threat of electric shock revealed by spatially-filtered magnetoencephalography

Brian R. Cornwell[a,*], **Johanna M.P. Baas**[c], **Linda Johnson**[a], **Tom Holroyd**[b], **Frederick W. Carver**[b], **Shmuel Lissek**[a], and **Christian Grillon**[a]

[a]Mood and Anxiety Disorders Program, National Institute of Mental Health, 15K North Drive, MSC 2670, Bethesda, MD 20892, USA [b]MEG Core Facility, National Institute of Mental Health, Bethesda, MD, USA [c]Department of Psychonomics, Utrecht University, Utrecht, The Netherlands

Abstract

Stimulus novelty or deviance may be especially salient in anxiety-related states due to sensitization to environmental change, a key symptom of anxiety disorders such as posttraumatic stress disorder (PTSD). We aimed to identify human brain regions that show potentiated responses to stimulus deviance during anticipatory anxiety. Twenty participants (14 men) were presented a passive oddball auditory task in which they were exposed to uniform auditory stimulation of tones with occasional deviations in tone frequency, a procedure that elicits the mismatch negativity (MMN) and its magnetic counterpart (MMNm). These stimuli were presented during threat periods when participants anticipated unpleasant electric shocks, and safe periods when no shocks were anticipated. Neuromagnetic data were collected with a 275-channel whole-head MEG system and event-related beamformer analyses were conducted to estimate source power across the brain in response to stimulus deviance. Source analyses revealed greater right auditory and inferior parietal activity to stimulus deviance under threat relative to safe conditions, consistent with locations of MMN and MMNm sources identified in other studies. Structures related to evaluation of threat, left amygdala and right insula, also showed increased activity to stimulus deviance under threat. As anxiety level increased across participants, right and left auditory cortical as well as right amygdala activity increased to stimulus deviance. These findings fit with evidence of a potentiated MMN in PTSD relative to healthy controls, and warrant closer evaluation of how these structures might form a functional network mediating sensitization to stimulus deviance during anticipatory anxiety.

During a state of behavioral inhibition, stimulus novelty or deviance may be especially salient, driving an organism into an extremely cautious stance and poised to activate fight—flight mechanisms based on further evaluation of the perceived danger (Blanchard et al., 2001; Gray, 1982; Gray and McNaughton, 2000). Heightened responses to stimulus novelty may be governed by mechanisms related to sensitization processes in clinical anxiety disorders such as post-traumatic stress disorder (PTSD, American Psychiatric Association, 2000; Siegmund and Wotjak, 2006). This study aimed to identify human brain regions that show enhanced responses to stimulus deviance during a state of anticipatory anxiety. We studied this context-specific, increased salience of stimulus deviance in humans by using an instructed threat paradigm in which periods of potential threat (i.e., unpredictable electric shocks) and periods

*Corresponding author. Fax: +1 301 594 9959. *E-mail address:* E-mail: cornwellb@mail.nih.gov (B.R. Cornwell)..

of safety were explicitly defined (Grillon, 2002; Grillon et al., 2004). To characterize the neural structures involved in sensitization to stimulus deviance, we used spatially-filtered magnetoencephalography (MEG) or adaptive beamformer analyses to estimate the volumetric distribution of source power across the brain (Hillebrand et al., 2005; Robinson and Vrba, 1999).

Our procedure consisted of a passive oddball auditory task in which participants were exposed to uniform auditory stimulation of pure tones with occasional changes in tone frequency (i.e., frequency deviants). This type of procedure elicits the classical mismatch negativity (MMN) and its magnetic counterpart (MMNm), a large deflection in evoked activity that peaks between 150 and 250 ms after the onset of the deviant stimulus (for reviews, see Naatanen et al., 2005, Naatanen and Winkler, 1999). The MMN and MMNm are considered neural correlates of *preattentive* auditory discrimination or change detection as their properties are not changed by highly distracting tasks such as watching a silent movie (Naatanen and Alho, 1995) or reading a magazine (Morgan and Grillon, 1999). Preattentive change detection may reflect the ability of the auditory system to automatically tune into and maintain the invariant qualities of the auditory environment (Cowan et al., 1993; Ritter et al., 1998; Ritter et al., 2002).

The underlying neural generators of the MMN and MMNm have been interrogated by dipole modeling studies of event-related potential and field data and functional magnetic resonance imaging (FMRI) studies. Dipole modeling has established that the primary generators of the MMN and MMNm lie in the superior temporal plane of both hemispheres, probably in secondary and/or higher order auditory association areas such as Brodmann Areas (BA) 42 and 22 (Giard et al., 1990; Rosburg, 2003; Sams and Hari, 1991; Scherg and Berg, 1991). Moreover, there is evidence of additional generators, particularly right-lateralized, in prefrontal and inferior parietal cortices that contribute to the MMN (Marco-Pallares et al., 2005) and MMNm (Levanen et al., 1996). FMRI studies corroborate these dipole modeling results in showing activity in temporal cortices (Doeller et al., 2003; Liebenthal et al., 2003; Opitz et al., 2002; Wible et al., 2001) as well as in right inferior frontal and inferior parietal cortices related to detection of stimulus deviance (Molholm et al., 2005; Opitz et al., 2002).

Morgan and Grillon (1999) reported evidence that women with PTSD exhibit a larger MMN than their healthy female counterparts with the same auditory stimuli under normal resting conditions. The authors attributed this potentiated response to the chronic hypervigilance central to the pathology of PTSD (American Psychiatric Association, 2000), which may sensitize patients to stimulus deviance. Because source analyses were not conducted, it is unknown whether the primary MMN generators showed elevated activity in the PTSD group compared to the control group and/or whether additional generators, from regions not typically involved in the MMN, contributed to group differences in the scalp-recorded potentials. Moreover, it is not conclusive whether the potentiated MMN can be causally attributed to the pathological condition or to stable individual differences in anxious reactivity that existed before onset of clinical status. Supporting this latter possibility, Hansenne et al. (2003) showed that MMN amplitude is positively correlated with individual differences in harm avoidance, an aspect of one's temperament that is related to behavioral inhibition.

We addressed these issues by exposing healthy participants to instances of stimulus deviance under a threat condition in which they anticipated aversive shocks and under a safe condition. Event-related beamformer analyses were conducted to estimate distributions of evoked activity across the brain to stimulus deviance under threat and safe conditions (Cheyne et al., 2006; Robinson, 2004). We hypothesized that, under threat of unpredictable shocks, healthy participants would exhibit potentiated neural responses to stimulus deviance in regions associated with the resting MMNm (e.g., superior temporal gyrus, BA 22/42). Because frequency deviants tend to preferentially activate right auditory cortical processes (Levanen et

al., 1996; Molholm et al., 2005), we predicted that modulatory effects of anticipatory anxiety on the response to deviant auditory tones would be primarily localized to the right temporal and inferior parietal cortices. It was also hypothesized that there would be recruitment of deeper structures involved in behavioral inhibition and evaluation of threat signals (e.g., amygdala) to deviant auditory stimuli under threat of shock.

Materials and methods

Participants

Twenty healthy individuals (14 men, mean age = 28 years) participated in a single MEG session followed by an MRI session to obtain an anatomical image. Five additional participants were excluded from analysis due to equipment failure and/or excessive head movement during the MEG recording. This study was approved by the National Institute of Mental Health Institutional Review Board and all participants gave informed consent prior to participation. Participant exclusion criteria included the following: (1) past or current psychiatric disorders as per Structured Clinical Interview for DSM-IV (First et al., 1995), (2) a medical condition that interfered with the objectives of the study per physical exam (e.g., tachycardia), (3) current use of psychoactive medications as per self-report, and (4) current use of illicit drugs determined by urine analysis.

Design and procedure

Three types of pure tones were presented binaurally via plastic tubes inserted into each ear: a standard 1000 Hz tone presented with a probability of 0.80 and two deviant frequency tones (936 and 1036 Hz), each with a probability of 0.10. Standard and deviant tones occurred at a rate of approximately 2 Hz in a pseudorandom order so that at least three standard tones were presented between deviant tones and that high and low frequency deviant tones alternated. Epochs for high and low frequency deviant tones were collapsed for the following source analyses.

In each of two runs, tones were presented to participants during alternating 30-s periods (10 times per run) in which participants were either threatened with electric shocks (threat condition) or safe from the shocks (safe condition). The order of the conditions was counterbalanced across participants. At the start of each period, participants were instructed vocally that shocks could be delivered unexpectedly at any point during the threat period (i.e., ‘shock at any time in the next 30 seconds’), or that shocks would not be delivered at any point during the safe period (i.e., ‘no shock at any time in the next 30 seconds, you are safe’).

A single shock was delivered by a constant current stimulator with two surface electrodes attached to the right or left wrist of every participant at the end of the last threat period in the first run only. Shock intensity was set for each participant before the first run using a work-up procedure that identified individual intensity levels that were reported to be moderately uncomfortable, but not painful. Participants were told that they would receive 1–5 shocks during the recordings. Such a procedure has been shown to elicit reliable physiological signs and subjective reports of anxiety in most participants (Grillon, 2002; Grillon et al., 2004). At the end of each run, participants verbally reported on a Likert-based scale how much overall anxiety (0–10, no anxiety—highly anxious) they felt, on average, during threat and safe periods.

Data acquisition

Neuromagnetic data were collected at 600 Hz (bandwidth: 0–150 Hz) with a CTF 275-channel whole-head system (VSM MedTech Ltd., Canada) in a magnetically shielded room (Vacuumschmelze, Germany) using active noise cancellation (i.e., synthetic 3rd gradient

balancing). Three electrical coils were attached to the nasion, left preauricular and right preauricular sites of each participant. Fiducial coils were energized before and after each run to localize the participant's head with respect to the MEG sensors. Total head displacement was measured after each run and could not exceed 5 mm for inclusion into the source analyses.

In a follow-up session, we obtained a high resolution T1-weighted anatomical image (FOV = 24, 1.2 mm axial slices, matrix = 256 × 256 × 128) with a 3-Tesla whole-body scanner (GE Signa, Milwaukee, WI). Radiology markers (IZI Medical Products, Baltimore, MD) were attached to these same sites for the anatomical MRI scan to facilitate spatial coregistration of the MRI and MEG data.

Event-related beamformer analysis

We extracted 100 epochs (0–500 ms post tone onset) for deviant tones and 100 epochs for standard tones for each condition and run (100 × 2 × 2 × 2 = 800 total epochs). Standard tone epochs included only those immediately preceding a deviant frequency tone. For each run, a single covariance matrix for constructing beamformer weights was computed on these unaveraged epochs following deviant and standard tones with a wide bandwidth of 1–30 Hz. Beamformer weights were calculated with a vector lead-field calculation (Sekihara et al., 2001) in 5 mm steps across the volume, using a multi-sphere head model derived from individual participants' structural MRIs (based on brain shapes). Virtual time series data were averaged in the time domain and source activity was quantified as the $\log_{10}$ ratio of power in the 150–250 ms window following deviant tones relative to the same window following standard tones, consistent with the variability in latency of the MMNm (Naatanen et al., 2005). By directly contrasting two time windows of virtual data (i.e., deviant vs. standard), uncorrelated noise passed through the spatial filters is factored out of the resulting power ratios and therefore does not need to be explicitly estimated as done by other researchers using event-related beamformers (e.g.,Cheyne et al., 2006). It is also presumed that activity related to general auditory stimulus processing will cancel out, leaving estimates of source power related specifically to stimulus deviance. A $\log_{10}$ transformation was performed to control for outliers in the distribution of power ratios within a volume. A sliding window analysis, with 50% overlap, captured differential source power, before and after the MMNm latency range, over the 0–300 ms post-stimulus onset epoch ([0–100 ms], [50–150 ms],…, [200–300 ms]). Contrasts were always made between corresponding time windows of deviant and standard epochs.

Group analyses were done in AFNI (Cox, 1996) after averaging volumes across runs, transforming individual averaged volumes into a common Talairach coordinate space, and normalizing voxel statistics within each source volume by scaling to the standard deviation. Normalizing volumetric statistics reduces the influence of global power variability across participants, which may otherwise bias local source power estimates. One-sample *t* tests were conducted on power ratios against a test case of zero (i.e., H_o: deviant power = standard power, or deviant-to-standard power ratio = 1) to define functional regions of interest (ROIs) per time window, selecting those voxels showing a greater response to deviant over standard tones in either the threat or safe condition at an alpha level <0.05 (uncorrected). This first step served to substantially reduce the number of voxels upon which comparisons were made between threat and safe conditions. Accordingly, within these ROIs exclusively, we performed paired *t* tests contrasting source power ratios between threat and safe conditions for each time window. We defined as differentially greater activation by threat relative to safe conditions clusters of at least 2 contiguous voxels with an average Student *t* statistic exceeding an alpha level of 0.05.

Nonparametric Spearman correlation analyses were conducted to identify activations within the ROIs showing positive correlations with self-reported anxiety levels across threat and safe conditions. Difference volumes (threat condition minus safe condition) were generated and

modeled against self-reported anxiety difference scores (threat minus safe self-reported anxiety). Again, we defined as statistically significant correlated activations clusters of at least 2 contiguous voxels in spatial extent with an average Spearman *r* statistic exceeding an alpha level of 0.05. Note that the use of spatial extent to define significant activations was arbitrary in both analyses and served the practical purpose of simplifying the results.

Results

Subjective anxiety

A 2 (condition) × 2 (run) repeated-measures ANOVA revealed a main effect of condition on self-reported anxiety, $F(1, 19)= 47.96$, $p<0.001$, but no main effect of run or condition by run interaction, Fs<1. Participants reported more anxiety during the threat of shock condition (mean±S.E.M., 4.65±0.56) relative to the safe condition (0.60±0.25). Three participants reported equal anxiety across the threat and safe conditions, with 2 reporting zero anxiety levels in both conditions. These participants were excluded from the following source analyses that focused on how anticipatory anxiety modulated neural responses to stimulus deviance.

Event-related beamformer analyses

Table 1 lists structures exhibiting a differential response to stimulus deviance between threat of shock and safe conditions across five time windows relative to stimulus onset. In the earliest time window (0 to 100 ms), enhanced responses to stimulus deviance under threat of shock were primarily found in posterior regions of the brain including several local maxima in the cerebellum. Left amygdala activation was also observed in the earliest time window but appeared to increase between 50 and 150 ms (Fig. 1). After 100 ms, there was evidence of right auditory cortical activation, particularly in BA 22 and BA 42, with the former peaking earlier than the latter (Fig. 2). Inferior parietal, precentral gyral and insular cortical activations were also found in the right hemisphere after 100 ms. Several activations related to stimulus deviance were observed in the left hemisphere after 100 ms: middle temporal cortical, superior frontal gyrus, inferior frontal gyrus, precuneus, and dorsomedial prefrontal cortical activations. We also found that no auditory cortical regions in either hemisphere showed greater activity to stimulus deviance in the safe relative to threat condition.

Regions showing greater differential activity in the threat of shock condition that were positively correlated with differential anxiety levels are presented in Table 2. These regions were predominantly right-lateralized in the early windows and then left-lateralized in the later windows. Superior temporal structures in both hemispheres showed positive correlations with anxiety level, including BA 41 (extending into inferior parietal cortex) in the right hemisphere and BA 22 in the left hemisphere (Figs. 3A—B). Two notable medial temporal structures, right amygdala and left posterior parahippocampal gyrus (extending into the cerebellum), also showed greater differential activity across threat and safe conditions that was related to a greater differential anxiety level (Figs. 3C—D).

Discussion

We studied neural responses to auditory stimulus deviance in healthy participants during a state of anticipatory anxiety. Anticipatory anxiety was generated by informing participants that they could receive electric shocks at any time during 30-s threat periods but not during 30-s safe periods. Under both conditions, participants were presented repetitive pure tones in which occasional frequency deviants were embedded. Event-related beamformer analyses were conducted to estimate the volumetric distribution of source power across the brain, to primarily identify regions showing potentiated responses to stimulus deviance under threat of shock. Based on findings in PTSD of a larger MMN than healthy controls under normal resting

conditions (Morgan and Grillon, 1999), we hypothesized that right auditory cortical regions would show greater activity to stimulus deviance in healthy participants under threat of shock than safe conditions, accompanied by activity in structures related to evaluation of threat. Results yielded support for both of these hypotheses.

Source analyses revealed greater right superior temporal (BA 22, 42) and inferior parietal cortical activations to frequency deviants as participants anticipated unpredictable electric shocks compared to safe conditions (Fig. 2). These activations peaked 150–300 ms following the onset of the deviant auditory tones consistent with the temporal properties of the MMN and MMNm, and their locations generally fit with previous dipole modeling studies of the MMN and MMNm and related FMRI studies finding primarily right temporal and parietal cortical sources (Levanen et al., 1996;Marco-Pallares et al., 2005;Molholm et al., 2005;Opitz et al., 2002). Further, there is evidence from human intracranial recordings suggesting that BA 42 is the primary substrate mediating echoic memory processes and BA 22 is involved in integrating these memory processes with new afferent signals (Kropotov et al., 2000;Liasis et al., 1999). Our results suggest that these components of the neural substrate of the MMN and MMNm did, indeed, show potentiated responses under threat of shock conditions, suggesting a common interpretation to the finding in PTSD (Morgan and Grillon, 1999). Heightened vigilance, whether by experimentally-induced anxiety or by chronic anxiety, sensitizes the individual to changes in the auditory environment, which may in turn facilitate auditory discriminative processes.

While threat of shock elevated right auditory cortical activity to stimulus deviance more uniformly across participants, correlation analyses showed that activity in the left auditory cortices was governed more by individual differences in anxiety level. Those who reported greater differential anxiety in the threat condition relative to the safe condition tended to show a greater differential response in auditory association areas (BA 22) in the left hemisphere, although only in the few most anxious participants were there greater responses to stimulus deviance under threat than safe. This same relationship was true for right auditory structures (BA 41) prior to 150 ms post-stimulus onset, suggesting that higher anxiety levels were associated with earlier engagement of right auditory processes under threat. A modulation of early auditory processes by threat of shock is not unprecedented as auditory brainstem potentials have been shown to be potentiated by a very similar manipulation of anticipatory anxiety (Baas et al., 2006). In the current study, participants reported, on average, a medium anxiety level to threat of shock. We would predict, by extrapolation of the observed relationships, that a stronger manipulation of threat might reveal a more bilateral pattern of potentiated auditory cortical responses to stimulus deviance.

Source analyses revealed two activations that suggest stimulus deviance reflected a more salient, potentially threatening event under threat of shock: an early left amygdala activation and later right insular activation. Both of these structures have been implicated in central regulation of aversive-motivational processes, and shown to be activated during a similar instructed threat procedure (Phelps et al., 2001). Whereas the amygdala plays a critical role in evaluation of threat and initiation of behavioral and autonomic components of fear responses (Davis, 1992; LeDoux, 2000), the posterior insula is a major cortical structure that receives visceral feedback and processes pain signals from peripheral systems (Peyron et al., 2000; Sawamoto et al., 2000). These results indicate that healthy participants might be reacting to a change in auditory stimulation under threat of shock as a potential signal of imminent shock delivery, leading to the triggering of anticipatory processes related to pain. We should note that the reliability by which MEG can capture signals from relatively deep sources, such as the amygdala, is not currently known. Recent MEG studies using adaptive beamformers (Luo et al., 2007) and inverse source methods (Ioannides et al., 2000; Moses et al., 2007) have presented credible empirical evidence by using tasks that are known to involve the amygdala (e.g., facial

expression processing, Pavlovian fear conditioning; Adolphs, 2002; Davis 1992). Nevertheless, the current findings based on event-related beamformer analyses require replication.

Not only did we observe an early left amygdala response to stimulus deviance, we also found some evidence of a right amygdala response in the more anxious participants. Correlation analyses revealed both right amygdala activity and left posterior parahippocampal gyral activity to be positively correlated with self-reported anxiety, further suggesting activation of systems related to evaluation of threat to stimulus deviance in the threat condition (Figs. 3C—D). Interestingly, these correlations emerged in the later time windows (i.e., after 150 ms), suggesting that these structures were engaged in the more anxious participants only after stimulus deviance was detected. On the contrary, the left amygdala activation was observed early enough (i.e., 50–150 ms) to be potentially contributing to the greater auditory cortical response under threat of shock. We have no evidence bearing on this issue, but leave it as an important issue to be addressed in the future by studying the linear and nonlinear synchronization of activity across these regions.

An intriguing aspect of activation of structures involved in evaluation of threat stems from the fact that there was no relationship between the type of auditory stimuli and the shock. The pattern of neural responses exhibited during threat of shock suggests that deviant stimuli were treated as potentially meaningful events. It would be highly adaptive that neural mechanisms involved in the early detection of environmental changes increase their sensitivity during a state of anticipatory anxiety. From an evolutionary perspective, the cost of overreacting to meaningless changes in the environment is little compared to the potential cost of missing a warning signal. This is a tentative interpretation of the present findings that no doubt requires further substantiation. Moreover, one of our underlying assumptions motivating this study is that threat of shock elicits a state of anticipatory anxiety in healthy participants that adequately models essential properties of chronic anxiety as seen in PTSD. While our results converge with Morgan and Grillon's (1999) finding in PTSD, it is critical that we establish a common set of structures that show potentiated responses to stimulus deviance in PTSD and in healthy participants under threat of shock. Finally, it is equally important to demonstrate with further research the interrelationships of these structures with the temporal unfolding of these neural processes to understand how this putative network mediates sensitization of stimulus deviance during a state of anticipatory anxiety.

Acknowledgment

This research was supported by the Intramural Research Program of the National Institute of Mental Health.

References

Adolphs R. Recognizing emotion from facial expressions: psychological and neurological mechanisms. Behav. Cogn. Neurosci. Rev 2002;1(1):21–62. [PubMed: 17715585]

American Psychiatric Association. Diagnostic and Statistical Manual of Mental Disorders (DSM-IV-TR). Vol. 4th edition. 2000.

Baas J, Milstein J, Donlevy M, Grillon C. Brainstem correlates of defensive states in humans. Biol. Psychiatry 2006;59(7):588–593. [PubMed: 16388780]

Blanchard CD, Hynd AL, Minke KA, Minemoto T, Blanchard RJ. Human defensive behaviors to threat scenarios show parallels to fear- and anxiety-related defense patterns of non-human mammals. Neurosci. Biobehav. Rev 2001;25:761–770. [PubMed: 11801300]

Cheyne D, Bakhtazad L, Gaetz W. Spatiotemporal mapping of cortical activity accompanying voluntary movements using an event-related beamforming approach. Hum. Brain Mapp 2006;27:213–229. [PubMed: 16037985]

Cowan N, Winkler I, Teder W, Naatanen R. Memory prerequisites of the mismatch negativity in the auditory event-related potential (ERP). J. Exp. Psychol.: Learn. Mem. Cogn 1993;19:909–921. [PubMed: 8345328]

Cox RW. AFNI: software for analysis and visualization of functional magnetic resonance neuroimages. Comput. Biomed. Res 1996;29:162–173. [PubMed: 8812068]

Davis M. The role of the amygdala in fear and anxiety. Ann. Rev. Neurosci 1992;15:353–375. [PubMed: 1575447]

Doeller CF, Opitz B, Mecklinger A, Krick C, Reith W, Schroger E. Prefrontal cortex involvement in preattentive auditory deviance detection: neuroimaging and electrophysiological evidence. NeuroImage 2003;20:1270–1282. [PubMed: 14568496]

First, MB.; Spitzer, RI.; Williams, JBW.; Gibbon, M. Structured Clinical Interview from DSM-IV (SCID). American Psychiatric Association; Washington, DC: 1995.

Giard MH, Perrin F, Pernier J, Bouchet P. Brain generators implicated in the processing of auditory stimulus deviance: a topographic event-related potential study. Psychophysiol 1990;27(6):627–640.

Gray, JA. The Neuropsychology of Anxiety: An Enquiry into the Function of the Septo-Hippocampal System. Oxford Univ. Press; Oxford: 1982.

Gray, JA.; McNaughton, N. The Neuropsychology of Anxiety. Vol. 2nd ed. Oxford University Press; Oxford: 2000.

Grillon C. Startle reactivity and anxiety disorders: aversive conditioning, context, and neurobiology. Biol. Psychiatry 2002;52(10):958–975. [PubMed: 12437937]

Grillon C, Baas JP, Lissek S, Smith K, Milstein J. Anxious responses to predictable and unpredictable aversive events. Behav. Neurosci 2004;118(5):916–924. [PubMed: 15506874]

Hansenne M, Pinto E, Scantamburlo G, Renard B, Reggers J, Fuchs S, Pitchot W, Ansseau M. Harm avoidance is related to mismatch negativity (MMN) amplitude in healthy subjects. Pers. Individ. Differ 2003;34(6):1039–1048.

Hillebrand A, Singh KD, Holliday IE, Furlong PL, Barnes GR. A new approach to neuroimaging with magnetoencephalography. Hum. Brain Mapp 2005;25:199–211. [PubMed: 15846771]

Ioannides AA, Liu LC, Kwapien J, Drozdz S, Streit M. Coupling of regional activations in a human brain during an object and face affect recognition task. Hum. Brain Mapp 2000;11:77–92. [PubMed: 11061335]

Kropotov JD, Alho K, Naatanen R, Ponomarev VA, Kropotova OV, Anichkov AD, Nechaev VB. Human auditory—cortex mechanisms of preattentive sound discrimination. Neurosci. Lett 2000;280:87–90. [PubMed: 10686384]

Lancaster JL, Woldorff MG, Parsons LM, Liotti M, Freitas CS, Rainey L, Kochunov PV, Nickerson D, Mikiten SA, Fox PT. Automated Talairach atlas labels for functional brain mapping. Hum. Brain Mapp 2000;10:120–131. [PubMed: 10912591]

LeDoux JE. Emotion circuits in the brain. Annu. Rev. Neurosci 2000;23:155–184. [PubMed: 10845062]

Levanen S, Ahonen A, Hari R, McEvoy L, Sams M. Deviant auditory stimuli activate human left and right auditory cortex differently. Cereb. Cortex 1996;6:288–296. [PubMed: 8670657]

Liasis A, Towell A, Boyd S. Intracranial auditory detection and discrimination potentials as substrates of echoic memory in children. Brain Res. Cogn. Brain Res 1999;7(4):503–506. [PubMed: 10076095]

Liebenthal E, Ellingson ML, Spanaki MV, Prieto TE, Ropella KM, Binder JR. Simultaneous ERP and fMRI of the auditory cortex in a passive oddball paradigm. NeuroImage 2003;19:1395–1404. [PubMed: 12948697]

Luo Q, Holroyd T, Jones M, Hendler T, Blair J. Neural dynamics for facial threat processing as revealed by gamma band synchronization using MEG. NeuroImage 2007;34(2):839–847. [PubMed: 17095252]

Marco-Pallares J, Grau C, Ruffini G. Combined ICA-LORETA analysis of mismatch negativity. NeuroImage 2005;25:471–477. [PubMed: 15784426]

Molholm S, Martinez A, Ritter W, Javitt DC, Foxe JJ. The neural circuitry of pre-attentive auditory change-detection: an fMRI study of pitch and duration mismatch negativity generators. Cereb. Cortex 2005;15:545–551. [PubMed: 15342438]

Morgan CA III, Grillon C. Abnormal mismatch negativity in women with sexual assault-related posttraumatic stress disorder. Biol. Psychiatry 1999;45(7):827–832. [PubMed: 10202569]

Moses SN, Houck JM, Martin T, Hanlon FM, Ryan JD, Thoma RJ, Weisend MP, Jackson EM, Pekkonen E, Tesche CD. Dynamic neural activity recorded from human amygdala during fear conditioning using magnetoencephalography. Brain Res. Bull 2007;71:452–460. [PubMed: 17259013]

Naatanen R, Alho K. Mismatch negativity—A unique measure of sensory processing in audition. Int. J. Neurosci 1995;80:317–337. [PubMed: 7775056]

Naatanen R, Winkler I. The concept of auditory stimulus representation in cognitive neuroscience. Psychol. Bull 1999;125:826–859. [PubMed: 10589304]

Naatanen R, Jacobsen T, Winkler I. Memory-based or afferent processes in mismatch negativity (MMN): a review of the evidence. Psychophysiology 2005;42:25–32. [PubMed: 15720578]

Opitz B, Rinne T, Mecklinger A, Von Cramon DY, Schroeger E. Differential contribution of frontal and temporal cortices to auditory change detection: fMRI and ERP results. NeuroImage 2002;15:167–174. [PubMed: 11771985]

Peyron R, Laurent B, Garcia-Larrea L. Functional imaging of brain responses to pain. Neurophysiol. Clin 2000;30:263–288. [PubMed: 11126640]

Phelps EA, O'Connor KJ, Gatenby JC, Gore JC, Grillon C, Davis M. Activation of the left amygdala to a cognitive representation of fear. Nat. Neurosci 2001;4(4):437–441. [PubMed: 11276236]

Ritter W, Gomes H, Cowan N, Sussman E, Vaughan HG Jr. Reactivation of a dormant representation of an auditory stimulus feature. J. Cogn. Neurosci 1998;10:605–614. [PubMed: 9802993]

Ritter W, Sussman E, Molholm S, Foxe JJ. Memory reactivation or reinstatement and the mismatch negativity. Psychophysiology 2002;39:158–165. [PubMed: 12212664]

Robinson SE. Localization of event-related activity by SAM(erf). Neurol. Clin. Neurophysiol 2004:109. [PubMed: 16012649]

Robinson, SE.; Vrba, J. Functional neuroimaging by synthetic aperture magnetometry. In: Yoshimine, T.; Kotani, M.; Kuriki, S.; Karibe, H.; Nakasato, N., editors. Recent Advances in Biomagnetism: Proceedings from the 11th International Conference on Biomagnetism; Sendai: Tokoku Univ. Press; 1999. p. 302-305.

Rosburg T. Left hemisphere dipole locations of the neuromagnetic mismatch negativity to frequency, intensity and duration deviants. Brain Res. Cogn. Brain Res 2003;16:83–90. [PubMed: 12589892]

Sawamoto N, Honda M, Okada T, Hanakawa T, Kanda M, Fukuyama H, Konishi J, Shibasaki H. Expectation of pain enhances responses to nonpainful somatosensory stimulation in the anterior cingulate cortex and parietal operculum/posterior insula: an event-related functional magnetic resonance imaging study. J. Neurosci 2000;20(19):7438–7445. [PubMed: 11007903]

Sekihara K, Nagarajan SS, Poeppel D, Marantz A, Miyashita Y. Reconstructing spatio-temporal activities of neural sources using an MEG vector beamformer technique. IEEE Trans. Biomed. Eng 2001;48:760–771. [PubMed: 11442288]

Sams M, Hari R. Magnetoencephalography in the study of human auditory information processing. Ann. N. Y. Acad. Sci 1991;620:102–117. [PubMed: 2035937]

Scherg M, Berg P. Use of prior knowledge in brain electromagnetic source analysis. Brain Topogr 1991;4:143–150. [PubMed: 1793688]

Siegmund A, Wotjak CT. Toward an animal model of posttraumatic stress disorder. Ann. N. Y. Acad. Sci 2006;1071:324–334. [PubMed: 16891581]

Wible CG, Kubicki M, Yoo SS, Kacher DF, Salisbury DF, Anderson MC, Shenton ME, Hirayasu Y, Kikinis R, Jolesz FA, McCarley RW. A functional magnetic resonance imaging study of auditory mismatch in schizophrenia. Am. J. Psychiatry 2001;158:938–943. [PubMed: 11384903]

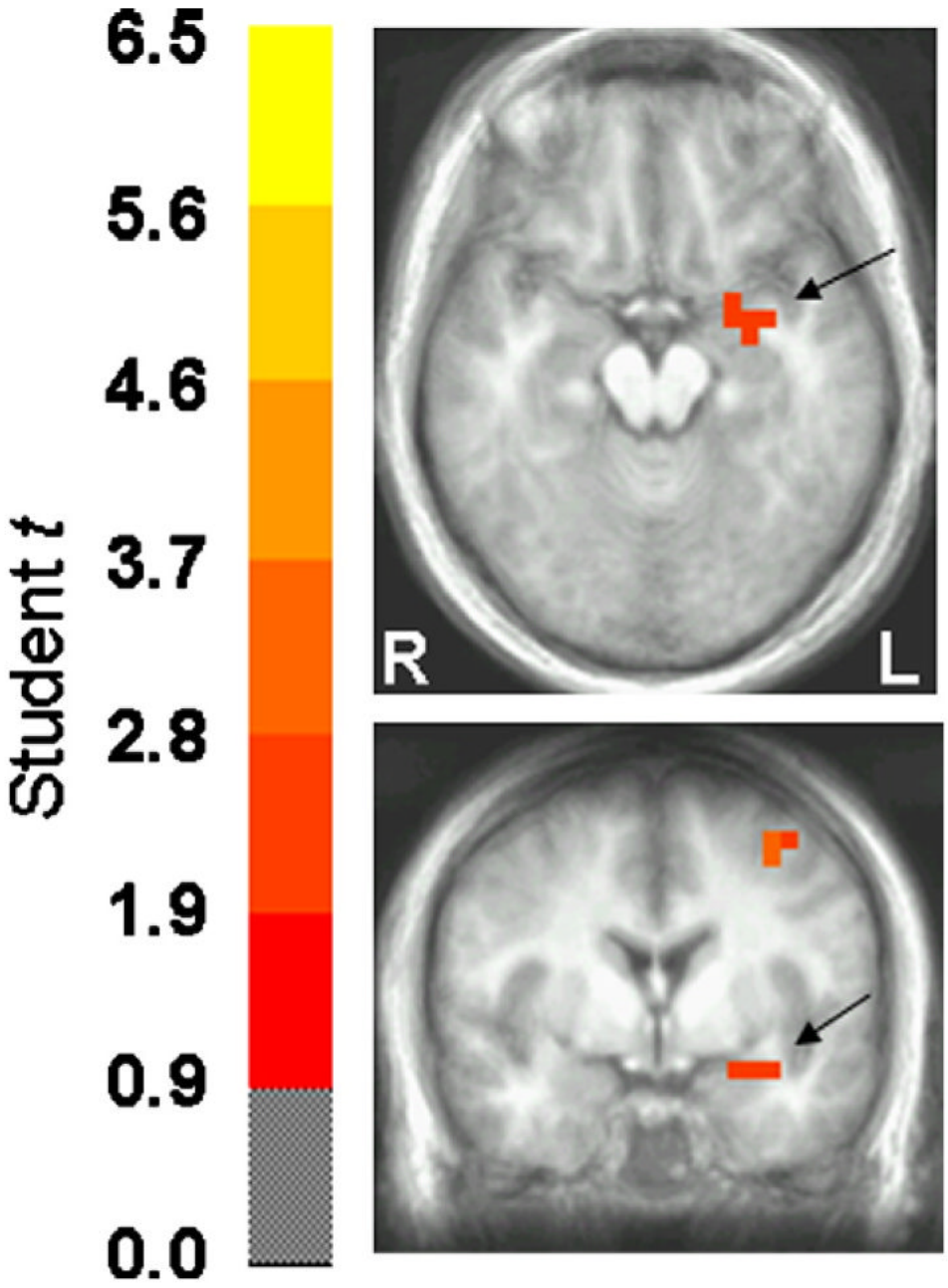

Fig. 1.

Paired *t* statistic volume of the threat-to-safe contrast in axial and coronal views and thresholded at $p<0.05$. Images are in radiological orientation (left=right, and vice versa). The center of the medial activation depicted in both views corresponds to the left amygdala according to the Talairach daemon (Lancaster et al., 2000). There was a greater left amygdala response to stimulus deviance under threat of shock relative to safe conditions between 50 and 150 ms post-stimulus onset.

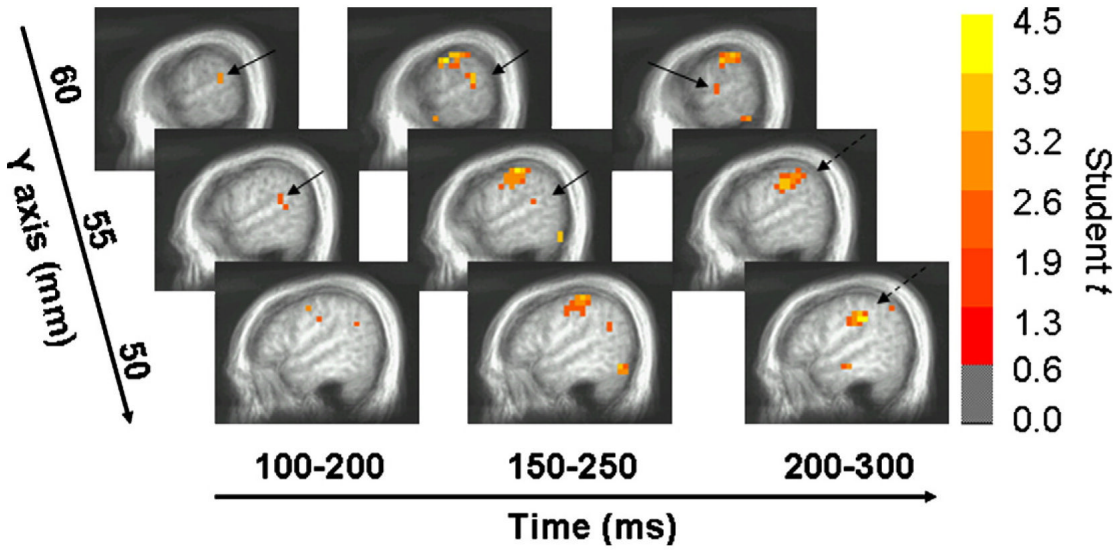

Fig. 2.

Sagittal views of the right hemisphere showing significant *t* statistics for the threat-to-safe contrast across time, thresholded at $p<0.05$ (uncorrected), overlaid on an averaged anatomical MRI. Images are in radiological orientation. Greater activity to stimulus deviance in the threat of shock condition was observed in right auditory regions such as BA 22 and BA 42 between 100 and 300 ms post-stimulus onset (solid arrows). Right inferior parietal cortical activity peaked between 200 and 300 ms (broken arrows).

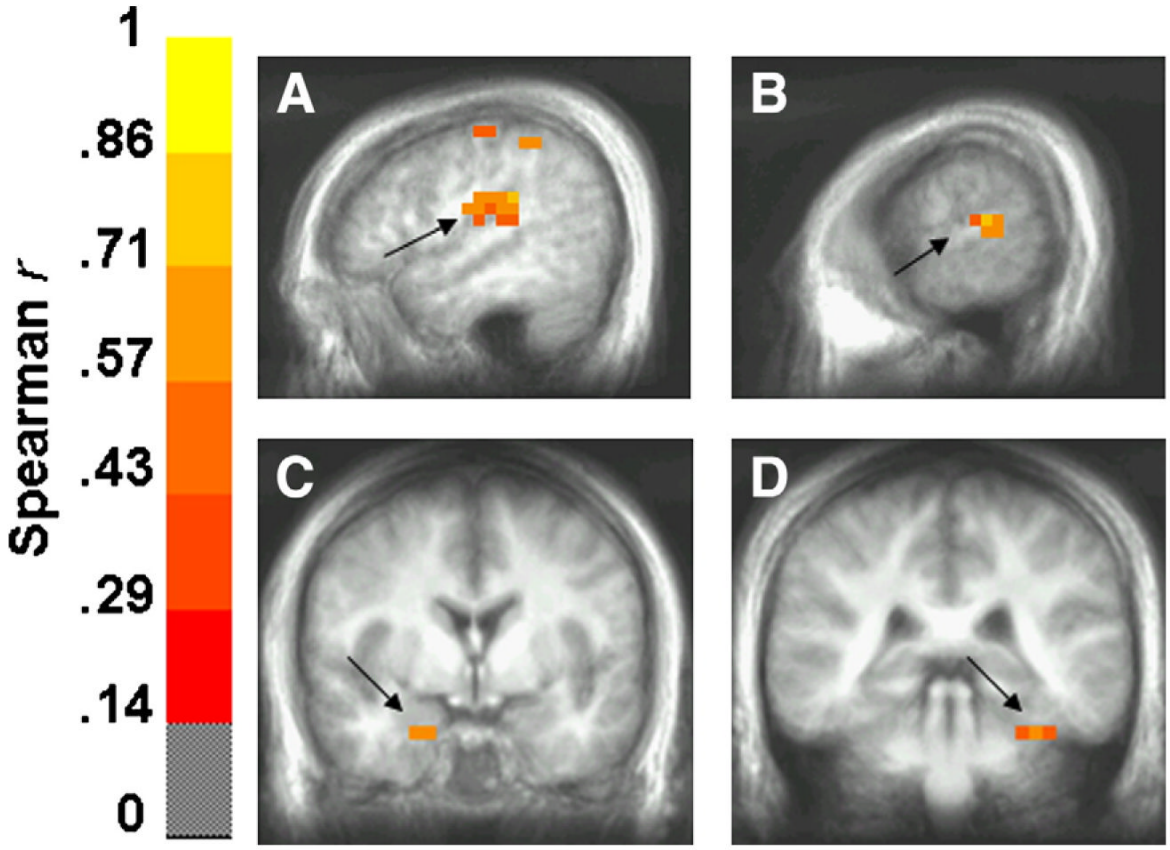

Fig. 3.

Spearman correlation coefficient volumes (thresholded at $p<0.05$) showing regions exhibiting a greater differential response to stimulus deviance under threat as a function of greater anxiety levels. Structures (indicated by solid arrows) showing this positive correlation included right inferior parietal lobule (BA 40, 41) between 50 and 150 ms (A), left superior temporal gyrus (BA 22) between 150 and 250 ms (B), right amygdala between 150 and 250 ms (C) and left parahippocampal gyrus/culmen between 200 and 300 ms (D). Images are in radiological orientation.

Table 1

Regions showing greater differential activation to stimulus deviance in threat of shock relative to safe conditions

Region	Side	Local maximum			
		x	y	z	Student *t*
0 to 100 ms					
Amygdala	L	-32	-2	-13	2.31
Culmen	L	-2	-57	-3	3.87*
Culmen	R	3	-52	-3	3.35*
Culmen, Lingual gyrus	L	-2	-62	2	3.00*
Inferior semi-lunar lobule	L	-27	-62	-43	2.72
Middle occipital gyrus, BA 37/19	R	48	-67	-8	2.38
Middle temporal gyrus, BA 37/19	R	48	-57	2	3.04*
50 to 150 ms					
Amygdala	L	-27	-2	-13	2.75
Parahippocampal gyrus, BA 36	L	-37	-22	-13	2.36
Middle frontal gyrus, BA 6	R	43	3	47	2.53
Middle frontal gyrus, BA 6	L	-32	-2	47	3.18*
Middle temporal gyrus, BA 21	R	58	-57	2	2.61
100 to 200 ms					
Middle frontal gyrus, BA 6	R	38	8	52	3.15*
Middle temporal gyrus, BA 21	L	-52	-22	-13	3.27*
Precentral gyrus, BA 6	R	38	-12	37	2.32
Precentral gyrus, BA 4	R	48	-7	42	3.19*
Superior frontal gyrus, BA 9	L	-32	48	27	2.48
Superior temporal gyrus, BA 22	R	58	-37	17	2.84
150 to 250 ms					
Fusiform gyrus, BA 37	R	48	-62	-13	3.57*
Inferior frontal gyrus, BA 45	L	-52	18	17	2.96*
Inferior parietal lobule, BA 40/22	R	58	-37	22	3.53*
Middle frontal gyrus, BA 6	R	38	13	47	2.26
Precentral gyrus, BA 6	R	58	-12	37	4.19**

Region	Side	Local maximum			
		x	y	z	Student *t*
Precuneus, BA 7	L	-22	-62	52	2.44
200 to 300 ms					
Fusiform gyrus, BA 37	R	58	-47	-18	2.65
Inferior parietal lobule, BA 40	R	48	-32	32	4.26**
Insula, BA 13	R	43	-17	-8	3.16*
Medial frontal gyrus, BA 8	L	-7	23	47	3.85*
Medial frontal gyrus, BA 6	R	3	-7	57	2.94*
Transverse temporal gyrus, BA 42	R	63	-17	12	3.09*

Regional activations were defined as at least 2 contiguous voxels with the probability of the average *t* statistic <0.05 (uncorrected). Coordinates are in Talairach space (in mm) and were identified based on the automated Talairach Daemon (Lancaster et al., 2000). BA=Brodmann Area.

* $p<0.01$ (uncorrected),

** $p<0.001$(uncorrected).

Table 2

Regions showing greater differential power as a function of greater differential self-reported anxiety in the threat of shock versus safe condition

Region	Side	Local maximum			
		x	y	z	R_S
0 to 100 ms					
Culmen	R	13	-57	-8	0.51
Superior frontal gyrus, BA 10	L	-17	68	7	0.62*
Superior parietal lobule, BA 7	R	33	-67	47	0.63*
Superior temporal gyrus, BA 41	R	38	-32	17	0.59
50 to 150 ms					
Cuneus, BA 18	R	8	-87	22	0.51
Inferior parietal lobule, BA 41	R	48	-32	22	0.73**
Inferior temporal gyrus, BA 21	R	58	-17	-18	0.53
Postcentral gyrus, BA 3	R	43	-17	52	0.60
100 to 200 ms					
Middle temporal cortex, BA 21	R	53	-22	-13	0.65*
Postcentral gyrus	R	48	-17	27	0.56
Postcentral gyrus, BA 40	R	43	-32	52	0.54
Postcentral gyrus, BA 3	L	-42	-22	62	0.50
Superior temporal gyrus, BA 22	L	-52	-27	7	0.65*
Supramarginal gyrus, BA 40	R	38	-47	32	0.63*
150 to 250 ms					
Amygdala	R	23	-2	-23	0.62*
Fusiform gyrus, BA 37	L	-27	-42	-13	0.55
Inferior frontal gyrus, BA 45	L	-32	28	7	0.63*
Inferior temporal gyrus, BA 20	L	-57	-37	-18	0.55
Precuneus	R	18	-67	62	0.53
Precuneus, BA 31	R	18	-62	27	0.54
Superior temporal gyrus, BA 22	L	-62	-32	12	0.74**
200 to 300 ms					
Angular gyrus, BA 39	L	-47	-72	37	0.65*

Region	Side	Local maximum			
		x	y	z	R_S
Declive	R	13	-67	-13	0.62*
Inferior frontal gyrus, BA 46	L	-52	38	12	0.72*
Inferior parietal lobule, BA 40	R	48	-42	47	0.49
Inferior temporal gyrus, BA 20	L	-62	-17	-18	0.72*
Middle frontal gyrus, BA 8	L	-42	23	47	0.60
Middle occipital gyrus, BA 19	L	-47	-82	12	0.60
Parahippocampal gyrus/Culmen	L	-37	-37	-23	0.64*
Precuneus, BA 7	L	-2	-72	52	0.60
Precuneus, BA 7	L	-22	-72	37	0.57
Superior occipital gyrus, BA 39	L	-47	-77	27	0.64*

Regional activations were defined as at least 2 contiguous voxels with the probability of the average correlation coefficient <0.05 (uncorrected). Coordinates are in Talairach space (in mm) and were identified based on the automated Talairach Daemon (Lancaster et al., 2000). BA=Brodmann Area. R_S =Spearman correlation coefficient

*p<0.01 (uncorrected),

**p<0.001 (uncorrected).